Infrared Reflection-Absorption of Melittin Interaction with Phospholipid Monolayers at the Air/Water Interface

C. R. Flach,* F. G. Prendergast,‡ and R. Mendelsohn*

*Department of Chemistry, Newark College, Rutgers University, Newark, New Jersey 07102, and ‡Department of Biochemistry and Molecular Biology, Mayo Foundation, Rochester, Minnesota 55905 USA

ABSTRACT The interaction of melittin with monolayers of 1,2-dipalmitoylphosphatidylcholine and 1,2-dipalmitoylphosphatidylserine has been investigated with infrared external reflection-absorption spectroscopy. Improved instrumentation permits determination of acyl chain conformation and peptide secondary structure in situ at the air/water interface. The IR frequency of the 1,2-dipalmitoylphosphatidylcholine antisymmetric acyl chain CH_2 stretching vibration decreases by 1.3 cm^{-1} upon melittin insertion, consistent with acyl chain ordering, whereas the same vibrational mode increases by 0.5 cm^{-1} upon peptide interaction with the 1,2-dipalmitoylphosphatidylserine monolayer, indicative of chain disordering. Thus the peptide interacts quite differently with zwitterionic compared with negatively charged monolayer surfaces. Melittin in the monolayer adopted a secondary structure with an amide I(I') frequency (1635 cm^{-1}) dramatically different from the α-helical motif (amide I frequency 1656 cm^{-1} in a dry or H_2O hydrated environment, amide I' frequency 1645 cm^{-1} in an H→D exchanged α-helix) assumed in bilayer or multibilayer environments. This work represents the first direct in situ spectroscopic indication that peptide secondary structure in lipid monolayers may differ from that in bilayers.

INTRODUCTION

Melittin, the main component of bee venom (50% of its dry weight), is a cationic, amphiphilic, 26-amino acid peptide, widely employed as a paradigm for protein-lipid interaction. The peptide serves as a model for ion channel-forming proteins as it is found to induce voltage-dependent ion conductance (Smith et al., 1994). Melittin also induces many membrane-based phenomena, including cell lysis, fusion, and the activation of phospholipase A_2 and adenylate cyclase (Okada et al., 1994).

An understanding of the method of action of melittin in a lipidic environment requires the determination of its conformation, aggregation state, location, and orientation within the bilayer. Many spectroscopic studies of the structure of melittin in membranes suggest that the peptide adopts a predominantly α-helical secondary structure, with an interruption of same around residues 11–12 due to the presence of Pro-14 as a helix breaker (Dempsey, 1990, and references therein). Although a clear consensus does not exist, infrared (IR) spectroscopic studies have generally been consistent with the idea that under conditions of low hydration the helical portion of melittin is perpendicular to the bilayer plane, whereas under conditions of high hydration it is parallel (Vogel et al., 1983; Brauner et al., 1987; Frey and Tamm, 1991). In contrast, NMR investigations of Smith et al. (1994) suggest a transmembrane orientation of the helical portions of melittin in a hydrated system. Whether melittin interacts with lipid bilayers as a monomer or a tetramer depends upon the peptide-lipid ratio and the peptide environment (Hermetter and Lakowicz, 1986; Dempsey, 1990; John and Jahnig, 1991; Weaver et al., 1992; Okada et al., 1994). The peptide induces a change in lipid headgroup conformation, possibly leading to a volume expansion in the surface region (Smith et al., 1992; Dempsey, 1990; Dufourc et al., 1986). This expansion can be accommodated by lipids through an increase in acyl chain disorder.

Along with its interaction with lipid bilayers, melittin has strong surface activity at the A/W interface, resulting in stable monolayers (Birdi et al., 1983). Birdi and Gevod (1987) employed surface pressure (π) and surface potential measurements to compare the interactions of melittin with anionic versus cationic surfactants. Stronger interactions were found with the anionic monolayer, a consequence of the six positive charges possessed by the peptide. Ohki et al. (1994) conducted adsorption experiments with egg phosphatidylcholine (PC) and bovine brain phosphatidylserine (PS) monolayers. In contrast to prior results, they observed greater changes in pressure for the PC monolayer upon melittin adsorption compared with PS, possibly because of the presence of unsaturated acyl chains. In conjunction with vesicle electrophoretic mobility, leakage, and fusion studies, they proposed that the electrostatic interaction between PS and melittin prevents peptide insertion into the hydrophobic portion of the lipid, whereas the zwitterionic PC permits greater access of the peptide to the hydrophobic core, thereby promoting insertion.

Ebara and Okahata (1993) studied the adsorption of melittin to fully saturated acyl chain phosphatidylethanolamine monolayers at initial surface pressures of 10 and 40 mN/m. Through changes in π and by the use of a quartz-crystal microbalance, their results indicate that melittin insertion occurs at 10 mN/m and that only adsorption to the

Received for publication 26 June 1995 and in final form 25 September 1995.

Address reprint requests to Dr. Richard Mendelsohn, Department of Chemistry, Rutgers University, 73 Warren Street, Newark, NJ 07102. Tel.: 201-648-5613; Fax: 201-648-1264; E-mail: mendelsohn@.hades.rutgers.edu.

0006-3495/96/01/539/08 $2.00

monolayer occurs at 40 mN/m. Sui et al. (1994) combined changes in surface pressure for monolayers and circular dichroism (CD) spectra of transferred films with fluorescence, CD, and Fourier transform-IR (FTIR) vesicle experiments to study conformational changes upon the insertion of melittin into saturated PCs and phosphatidic acid. An increase in the α-helical content was observed upon peptide insertion into mixed lipid systems.

One drawback with previous monolayer studies involving melittin is the absence of direct molecular structure information from the film in situ at the A/W interface, thus precluding determination of structural parameters such as lipid acyl chain configuration and peptide secondary structure. To address these issues, the current investigation reports in situ (at the A/W interface) infrared external reflection-absorption spectroscopy (IRRAS) studies from monolayers of 1,2-dipalmitoylphosphatidylcholine (DPPC) and 1,2-dipalmitoylphosphatidylserine (DPPS) before and after melittin adsorption. Recent advances from this laboratory (Flach et al., 1994; Pastrana-Rios et al., 1996) and others (Cornut et al., 1995; Pezolet and Labrecque, 1995) in IRRAS instrumentation provide the opportunity to detect vibrational modes from both the lipid and protein components of the film in situ at the A/W interface, under conditions of controlled surface pressure.

MATERIALS AND METHODS

Materials

DPPC, DPPS, and acyl chain perdeuterated DPPC (DPPC-d_{62}) were obtained from Avanti Polar Lipids (Alabaster, AL) and used without further purification. Melittin was synthesized by solid phase methods. The peptide sequence is Gly-Ile-Gly-Ala-Val^5-Leu-Lys-Val-Leu-Thr^{10}-Thr-Gly-Leu-Pro-Ala^{15}-Leu-Ile-Ser-Trp-Ile^{20}-Lys-Arg-Lys-Arg-Gln^{25}-Gln-NH_2.

EGTA (97% pure) and D_2O (99.9%) were purchased from Sigma Chemical Co. Double-distilled H_2O was used, and all other salts, buffers, and solvents were of the highest purity commercially available.

Experimental methods

Phospholipid samples were prepared by dissolving appropriate weights of the powdered lipids in a $CHCl_3$:MeOH (3:2, v:v) solution while stirring and gently warming, as needed. Melittin was dissolved (~1.0 mg/ml) in Tris(hydroxymethyl)-aminomethane hydrochloride buffer (10 mM Tris, 100 mM NaCl, 0.1 mM EGTA, pH ~7.4) solution.

Before use, all components of the surface balance in contact with the sample were cleaned by soaking for 15 min in a chromic acid solution (Chromerge; Fisher Scientific, Fairlawn, NJ) and exhaustively rinsed with double-distilled H_2O. The Pt Wilhelmy plate was roughened with sandpaper, rinsed, and flamed. The cleanliness of the surface balance and subphase were ensured before IRRAS measurements by cycling through the full range of surface area and aspirating the surface while at minimum surface area. When a constant surface tension value of 72 ± 1 mN/m was observed over the entire surface area range, prepared solutions were laid on the surface.

For all experiments, the trough was filled with a Tris buffer subphase (pH ~7.4 or in D_2O, pD ~7.4), and monolayers of DPPC, DPPC-d_{62}, or DPPS (usually ~15 μl of a 0.5 μg/μl solution) were spread on the surface. After allowing for solvent evaporation, films were compressed until the desired surface pressure was achieved. Before the melittin adsorption experiments, IRRAS spectra were acquired during the intermittent compression of a pure DPPC monolayer. Surface pressure was held constant as each spectrum was obtained. For the melittin adsorption experiments, phospholipid films were compressed until the desired surface pressure (either 10 or 20 mN/m) was achieved. Surface area was held constant throughout the remainder of the experiment. IRRAS spectra of the phospholipid monolayers were then acquired. The appropriate amount of melittin solution (usually ~50 μl) was injected into the subphase, using a long-needle syringe to pierce the monolayer at various points in the trough. Changes in surface pressure were monitored until a constant value was reached, and then additional time (~15 min) was allowed before IRRAS data collection. Experiments were conducted at room temperature.

IRRAS apparatus

The spectrometer used was a BioRad (Digilab) FTS 40A spectrometer (Cambridge, MA) equipped with an external narrow-band mercury-cadmium-telluride detector. Interferograms were collected at 4 cm^{-1} resolution at an angle of incidence centered at 45° (beam spread ±4°), apodized with a triangular function, and Fourier-transformed with one level of zero-filling to produce spectral data encoded at 2 cm^{-1} intervals. For the pure DPPC monolayer, 512 scans were co-added to produce IRRAS spectra. For the melittin adsorption experiments, the trough shuttle system was used (Flach et al., 1994), where a total of 128 scans were co-added in two cycles of 64 scans each, with sample and reference wells being aligned in the IR beam in an alternating fashion. A macro program written on the BioRad 3200 data station allowed for successive co-addition of scans to preexisting interferogram files. A delay time of 20 s between trough rotation and data acquisition was visually found to be necessary to stop motion and to smooth the surface. For a full description of the external optical components and miniaturized trough system, the reader is referred to Flach et al. (1993b, 1994).

When necessary, residual water vapor rotation-vibration bands were subtracted using an appropriate reference spectrum and manufacturer-supplied software. Data were transferred to a microcomputer, and further manipulation was performed using software written at the National Research Council of Canada. Baselines were flattened before frequency determination with a center of gravity routine.

RESULTS

IRRAS of DPPC

Typical IRRAS spectra of the CH_2 stretching region for a DPPC monolayer at various surface pressures are overlaid in Fig. 1. The symmetric and asymmetric CH_2 ($\nu_{sym}CH_2$ and $\nu_{asym}CH_2$) stretching modes are observed at ~2850 and ~2920 cm^{-1}, respectively, along with the asymmetric methyl stretch at ~2960 cm^{-1}. Increasing π leads to increased reflection absorption (RA) intensity. The spectrum with the weakest bands was acquired at a π of ~4 mN/m; the RA intensity of $\nu_{asym}CH_2$ was ~1 milliabsorbance unit (mAU). π was held at 47 mN/m during collection of the spectrum with the most intense bands; the RA of $\nu_{asym}CH_2$ is ~5 mAU. The increase in RA is predominantly due to an increase in the number of molecules in the IR beam; however, the RA of the CH_2 stretching modes is also sensitive to acyl chain orientation. A decrease in the average tilt angle of the acyl chains with respect to the surface normal results in an increase in the RA (Mendelsohn et al., 1995).

Downward shifts in wavenumber for the CH_2 stretching vibrations are evident as π increases, indicative of acyl chain *gauche* to *trans* isomerization (Snyder et al., 1982). $\nu_{asym}CH_2$ is observed at 2923 cm^{-1} and at 2917 cm^{-1} for

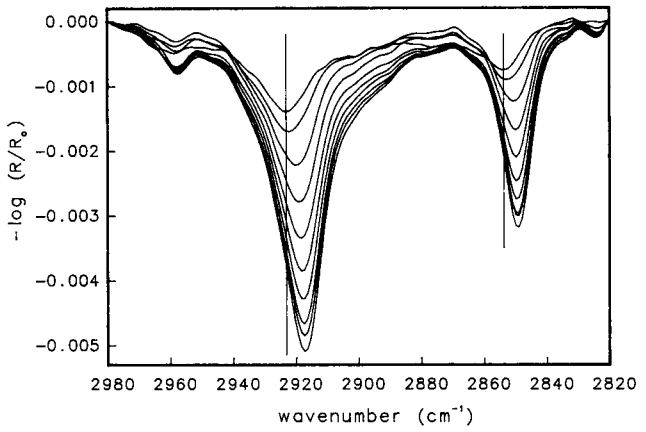

FIGURE 1 Overlaid IRRAS spectra of the methylene stretching region obtained during the intermittent compression of a DPPC monolayer on a buffered H_2O subphase (pH ~7.4). Data are plotted as $-\log (R/R_o)$, where R is the single-beam reflectivity spectrum from the film-covered surface and R_o is the same from the clean water surface. Surface pressure ranges from 4 to 47 mN/m from the least to most intense bands, respectively, at a pressure interval of ~5 mN/m. Vertical lines are drawn to emphasize the frequency downshift upon monolayer compression. Spectra are baseline corrected.

the lowest and highest surface pressures, respectively. The shift in frequency, typically used as a qualitative marker of acyl chain conformational order, indicates an increase in order with increasing π. This is consistent with previously reported IRRAS results that have been correlated with lipid phase transitions (Hunt et al., 1989).

IRRAS of DPPC/melittin and DPPS/melittin

Fig. 2 *A* and *B*, displays the $\nu_{asym}CH_2$ and $\nu_{sym}CH_2$ regions of the IRRAS spectra for DPPC and DPPS monolayers,

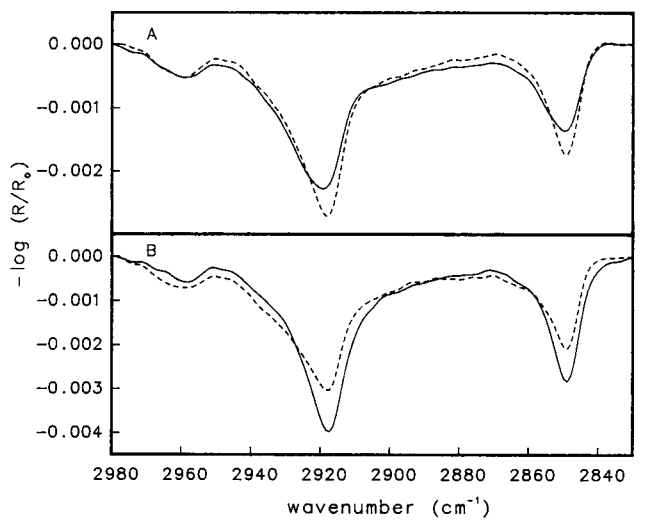

FIGURE 2 IRRAS spectra of the methylene stretching region for (*A*) DPPC and (*B*) DPPS monolayers on a buffered H_2O subphase before (*solid line*) and after (*dashed line*) melittin injection into the subphase. Spectra have been baseline corrected.

respectively, preceding and subsequent to melittin injection into a Tris buffer subphase. The difference in the response of the two lipids to peptide insertion is striking. Before the injection of melittin, the initial surface pressure (π_i) for both monolayers was ~10 mN/m. Upon addition of the same quantity of melittin to each subphase, the surface pressure was observed to increase rapidly (<2 min) to a final surface pressure (π_f) of 25 mN/m for the DPPC and to 37 mN/m for the DPPS monolayers. In response to peptide insertion, $\nu_{asym}CH_2$ of the DPPC monolayer is found to decrease by 1.3 cm^{-1}, whereas the same vibrational mode increases by 0.5 cm^{-1} for the DPPS monolayer (Table 1). The full width of this band at half-height (FWHH) decreases for DPPC, whereas an increase of comparable magnitude is observed for DPPS. Furthermore, the intensity of this mode increases for DPPC by 0.5 mAU (~20%) and decreases by 1 mAU (~25%) for DPPS upon melittin injection. Similar results are observed for $\nu_{sym}CH_2$.

IRRAS of DPPC-d_{62}/melittin

At a surface pressure of 10 mN/m, DPPC exists in a two-phase liquid expanded (disordered)/liquid condensed (more ordered) coexistence region, whereas DPPS is found in a liquid condensed or solid state (both substantially ordered), as determined by π-molecular area isotherms and IRRAS methylene stretching mode frequency shifts (Hunt et al., 1989; Flach et al., 1993a). To compare the response to melittin insertion of lipids initially in the same state, an acyl chain perdeuterated DPPC-d_{62} monolayer was spread and compressed to π_i of 20 mN/m (liquid condensed or solid state) before injection of the peptide into the subphase. The results are compared to those for a DPPC-d_{62} monolayer at a π_i of 10 mN/m and to a DPPS monolayer in the same physical state (Table 1). The supply of synthetic melittin was limited; thus substitution of DPPC for DPPC-d_{62} was undertaken so that these experimental results could be used as reference data for future studies of mixed monolayer films.

TABLE 1 Surface pressure and CH_2 (CD_2) asymmetric stretching band parameters in the presence and absence of subphase melittin

Lipid	Melittin (P/A)	Surface pressure (mN/m)	Frequency (cm^{-1})	FWHH (cm^{-1})	RA (mAU)
DPPC	A	9	2919.5	19.3	−2.1
DPPC	P	25	2918.2	16.4	−2.6
DPPS	A	10	2917.8	15.9	−3.8
DPPS	P	37	2918.3	19.3	−2.8
DPPC-d_{62}	A	10	2196.1	18.3	−0.6
DPPC-d_{62}	P	27	2194.4	17.3	−0.7
DPPC-d_{62}	A	20	2194.0	24.9	−1.2
DPPC-d_{62}	P	29	2193.6	22.7	−1.2

RA, reflection absorption intensity, i.e., $-\log R/R_o$; P, presence of subphase melittin; A, absence of subphase melittin.

Fig. 3, *A* and *B*, displays the CD_2 asymmetric and symmetric stretching regions ($\nu_{sym}CD_2$ and $\nu_{asym}CD_2$) for DPPC-d_{62} monolayers at a π_i of 10 mN/m on a D_2O subphase and at a π_i of 20 mN/m on an H_2O subphase, respectively. Before melittin injection, $\nu_{asym}CD_2$ of the monolayer at a π_i of 20 mN/m is observed at 2194.0 cm^{-1}, indicating substantially more order than the frequency (2196.1 cm^{-1}) noted for this monolayer at π_i of 10 mN/m. When melittin is injected into the subphase of the DPPC-d_{62} monolayer at the lower π_i, the pressure increase to π_f of 27 mN/m is very rapid (less than 1 min). In contrast, the increase in pressure from 20 to 29 mN/m required 5–10 min. The marked difference in the time course of the pressure changes for the two monolayers reflects the difference in the surface area available to the peptide in the two distinct physical states. At π_i of 10 mN/m, the presence of liquid expanded domains mixed among regions of a more condensed state allows for more rapid adsorption of the peptide compared to hindered adsorption induced by tighter lipid packing at a π_i of 20 mN/m.

The presence of melittin induced an ordering effect on the PC acyl chains for both surface pressures, as indicated by decreases in $\nu_{asym}CD_2$. The magnitude of the change, however, was much greater for DPPC-d_{62} at a π_i of 10 mN/m (~40% of the available range) than at a π_i of 20 mN/m (~10%). Upon melittin injection, an increase was observed in the RA of $\nu_{asym}CD_2$ for the monolayer at lower initial pressure, whereas the RA remained approximately the same for the higher pressure. It is of interest to note that the PC in the presence of melittin at a pressure of 27 mN/m is slightly less ordered than the PC in the absence of melittin at a lower pressure of 20 mN/m, indicating that an increase in pressure by compression may be more effective in ordering the acyl chains than the interaction of the monolayer with the peptide. This in turn suggests that a non-uniform surface may be presented to the lipid by the peptide, possibly permitting the formation of *gauche* rotations in the lipid acyl chains at the peptide/lipid interface.

A comparison of the IRRAS results for the DPPS and the DPPC-d_{62} (π_i = 20 mN/m) monolayers, both initially in a similar state of order, permits speculation concerning the effects of the lipid headgroup on the insertion properties of melittin. The anionic lipid monolayer undergoes a much greater increase in pressure than the zwitterionic monolayer upon melittin injection. Frequency changes of about the same magnitude are observed for both monolayers, but occur in opposite directions. The magnitude of the RA is observed to decrease upon peptide insertion for the PS monolayer but remains unchanged for the DPPC-d_{62} film.

Melittin secondary structure

Fig. 4, *A* and *B*, displays the lipid carbonyl (~1730 cm^{-1}), and peptide amide I (1680–1600 cm^{-1}) and II (~1550 cm^{-1}) regions of the IRRAS spectrum for melittin adsorbed to DPPS (π_i = 10 mN/m) before and after water vapor subtraction, respectively. Although a D_2O-based subphase was used, sharp water vapor bands (arising from both H_2O and HDO rotation-vibration bands) are pervasive throughout the spectrum in Fig. 4 *A*. Subtraction of water vapor is found to significantly reduce the interference without substantial modification to band position (Fig. 4 *B*). The amide

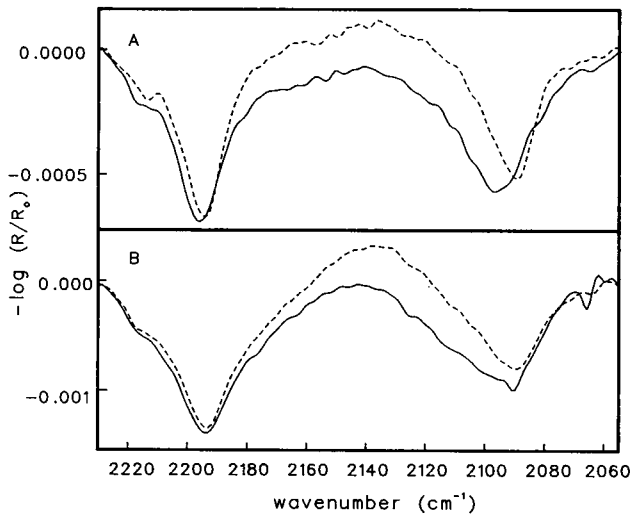

FIGURE 3 IRRAS spectra of the CD_2 stretching region for DPPC-d_{62} monolayers on (*A*) a D_2O buffer subphase at an initial surface pressure of 10 mN/m and (*B*) an H_2O buffer subphase at an initial pressure of 20 mN/m. Spectra are shown before (*solid line*) and after (*dashed line*) melittin injection. Water vapor absorbance bands are evident in the low wavenumber region of (*B*). Spectra have been baseline corrected.

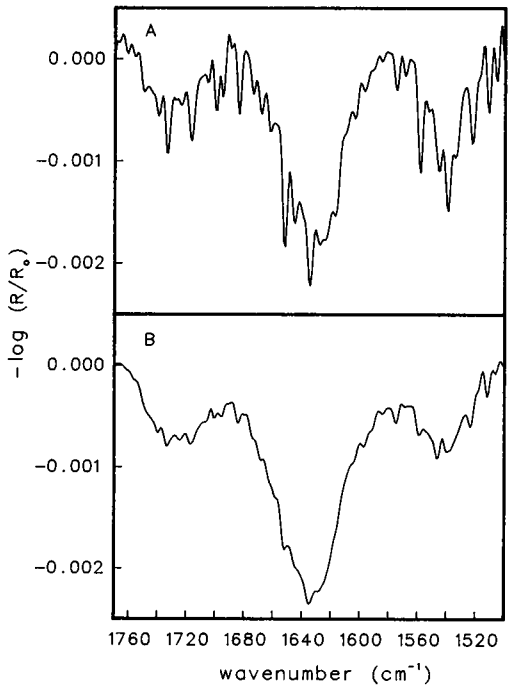

FIGURE 4 IRRAS spectra of the lipid carbonyl and amide I and II regions for the peptide melittin adsorbed to DPPS. (*A*) Original spectrum; (*B*) spectrum after water vapor was subtracted. The π after peptide adsorption was 37 mN/m. Spectra have been baseline corrected.

I (I′) band for the melittin/DPPS monolayer occurs at a frequency of ~1635 cm^{-1} with an intensity of ~2 mAU, whereas for a melittin/DPPC-d_{62} monolayer a frequency of ~1638 cm^{-1} with a RA of ~1 mAU is measured (Fig. 5). The larger RA value for the peptide adsorbed to the DPPS monolayer is consistent with the larger increase in surface pressure for this monolayer in the presence of protein when compared to either of the two PC monolayers at a π_i of 10 mN/m. The FWHH for the amide I band of melittin adsorbed to either the PS or PC monolayer is measured at ~43 cm^{-1}. Amide II bands are also present for both monolayers, indicating that H→D exchange is incomplete. An accurate determination of the frequency and intensity of the residual amide II is difficult because these are overlaid with sharp water vapor bands.

The lipid:peptide molar ratio for the DPPS monolayer is estimated at ~4 or 5 to 1 for the A/W interface, based on a comparison of the ratio of lipid carbonyl to amide I (I′) band intensities for the present monolayer and previously reported attenuated total reflectance IR (ATR-IR) studies (Brauner et al., 1987). The estimate must be considered with caution, however, as differences in extinction coefficients and orientation will affect intensities.

DISCUSSION

Before developments in IRRAS technology, it had been necessary to rely on techniques that provide no direct molecular structure information about the monolayer components upon protein insertion. Together with bulk phase studies, the approaches summarized in the introduction have provided some insight into possible mechanisms of interaction. However, results from CD and ATR-IR studies of transferred films must be considered with caution, in light of possible artifacts arising from film transfer from the A/W interface to solid substrates. The current experiments demonstrate the power of IRRAS to yield important structural information from monolayer components. Two results will be discussed in turn. First the effect of peptide on lipid monolayer organization will be considered. Second, the observation of a changed melittin secondary structure in lipid monolayers as compared to bilayers or multibilayers will be discussed.

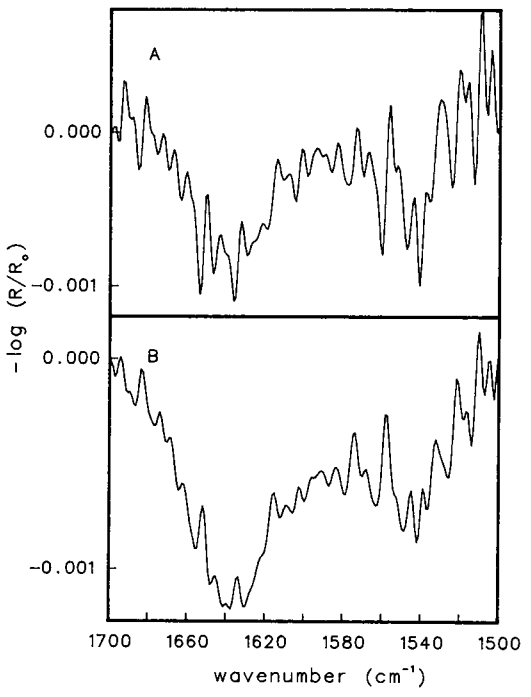

FIGURE 5 IRRAS spectra of the amide I and II regions for the peptide melittin adsorbed to DPPC. (*A*) Original spectrum; (*B*) spectrum after water vapor was subtracted. The π after peptide adsorption was 27 mN/m. Spectra have been baseline corrected.

Effects of melittin on lipid conformational order

Changes in π resulting from injection of a protein or peptide into the subphase are indicative of an interaction between the monolayer and the protein. Increases in π are assumed to result from protein penetration into the monolayer (Jones and Chapman, 1995). In the current experiments, increases in surface pressure were observed for both the DPPC and DPPS monolayers. The larger increase in surface pressure for the DPPS monolayer suggests a greater affinity of melittin for the anionic DPPS compared to the zwitterionic DPPC. Furthermore, the peptide induces only a small increase in the conformational order of the acyl chains in the DPPC-d_{62} monolayer at π_i of 20 mN/m, whereas the RA remains constant. When the PS and PC-d_{62} are both initially in relatively ordered states, melittin is observed to have a much greater effect on the PS monolayer. Both of these observations thus suggest an electrostatic component in melittin binding to membranes, consistent with some previous bulk phase (Batenburg et al., 1987b; Dempsey et al., 1989; Dufourc et al., 1986) and monolayer (Birdi and Gevod, 1987) studies, but in contradiction to the work of Ohki et al. (1994).

Hydrophobic interactions, thought to play a large role in the membrane lytic activity of melittin (Lafleur et al., 1989; Weaver et al., 1992), can be monitored through peptide-induced alterations of the lipid acyl chain CH_2 stretching frequencies. Changes in the spectral parameters of the acyl chain methylene vibrations are summarized in Table 1. The frequency shifts in the asymmetric stretching mode indicate that melittin induces *gauche* to *trans* isomerization, i.e., acyl chain conformational ordering, of the DPPC and disordering of the DPPS monolayers. Similarly, changes in the bandwidth, considered to be primarily sensitive to acyl chain mobility (Mendelsohn et al., 1981), indicate decreased motional rates for DPPC and increased motional rates for the DPPS acyl chains upon melittin adsorption.

Throughout the experiment, the number of lipid molecules per unit area on the surface exposed to the IR radiation and thus giving rise to the IRRAS intensity is constant. Upon peptide adsorption, changes in RA values therefore

arise only from changes in conformation and/or molecular orientation. The extent of conformational change is qualitatively monitored from the shifts in methylene stretching frequencies, while the dependence of the intensity on tilt angle of an ordered chain is such that a decrease in acyl chain tilt angle (toward the surface normal) results in an increase in the RA. For DPPC monolayers at π_i of 10 mN/m, the wavenumbers of the peptide-free film imply the presence of substantial chain disorder, whereas upon melittin insertion the peptide becomes rather highly ordered. It is difficult to distinguish between the fraction of the increase in RA due to the conformational ordering as revealed by the frequency decrease, and that due to a decrease in the average tilt angle of the chains.

For melittin adsorbed to the DPPS monolayer, although the frequency increase is slight (0.5 cm^{-1}) in this instance, a simple two-state model shows that it may nevertheless reflect a substantial decrease in conformational order, as calculated by Dluhy et al. (1983). We therefore again refrain from quantitative analysis of the intensity changes.

For the DPPC monolayers, an increase in conformational order is accompanied by a decrease in acyl chain rate motion as reflected in the decreased linewidth, similar to that occurring when a bulk-phase lipid dispersion is cooled through the liquid crystal → gel phase transition. For DPPS monolayers, melittin induces a decrease in conformational order and an increase in acyl chain motion, similar to the effects taking place when a lipid dispersion is heated.

Differing results are obtained when bulk, fluid-phase PC systems are compared with monolayers in the liquid expanded/liquid condensed (LE/LC) state. Melittin-induced acyl chain disordering is observed in the bulk phase (Brauner et al., 1987; Weaver et al., 1992), whereas the acyl chains in the monolayer display conformational ordering. The reason for the difference may be the presence of domains in the monolayer, where the peptide has the potential to selectively interact with the LE phase. This would lead to a reduction in the available area per DPPC molecule, creating more of the LC phase, consistent with both the decrease in frequency of $\nu_{asym}CH_2$ and the increase in π.

Surface pressure measurements and the RA values for the peptide suggest a greater degree of melittin insertion and interaction with the DPPS monolayer. This is consistent with tryptophan fluorescence studies on cardiolipin (negatively charged) versus phosphatidylcholine bulk phase systems (Batenburg et al., 1987a).

Melittin secondary structure in monolayer films

The observed amide I vibrational frequencies (~1638 cm^{-1} and ~1635 cm^{-1}) for the adsorbed peptide in mixed films with DPPC and DPPS, respectively, are far too low to arise from the predominantly α-helical secondary structure known to occur in bulk and multibilayer phases. An unexchanged α-helical amide I mode normally appears as a sharp feature (full width at half height ~15–25 cm^{-1}) near 1655 cm^{-1} and is shifted down by as much as 12 cm^{-1} upon complete H→D exchange, with an accompanying increase in bandwidth (40–50 cm^{-1}) (Flach et al., 1994; Zhang et al., 1992; Frey and Tamm, 1991). Also upon complete H→D exchange, the amide II frequency (1530–1550 cm^{-1}) is shifted into the 1450–1465 cm^{-1} range (Miyazawa et al., 1958).

Table 2 provides a summary of previously reported amide I (I′) frequencies for melittin in various environments. In accord with the above, Brauner et al. (1987) have observed an unexchanged melittin helical frequency of 1656 cm^{-1} upon its interaction with bilayers, whereas Frey and Tamm (1991) observed a frequency of 1645 cm^{-1} for melittin as a fully exchanged α-helix. Although random coil secondary structures may absorb IR radiation in the same spectral

TABLE 2 Summary of published melittin amide I (I′) frequencies

Sample	Physical state	Bulk phase	Method	Amide I ν (cm^{-1})	Amide II
DPPS:melittin (~5:1)*	Monolayer π_i = 10 mN/m	D_2O	IRRAS	1635	P‡
DMPC/DMPA (8/2):melittin (40:1)§	Vesicles at 45°	D_2O	FTIR	1651 1637 (sh)¶	Not shown
POPC/POPG (4:1):melittin‖	Single supported planar bilayer	D_2O	ATR-FTIR	1645	A
DPPC:melittin (10:1)**	Dry multilayer film	NA	ATR-FTIR	1656 1685 (sh)	P

* Current study.
‡ P and A represent present and absent, respectively.
§ Sui et al. (1994).
¶ sh represents shoulder.
‖ Frey and Tamm, (1991).
** Brauner et al., (1987).

regions as the α-helix, Frey and Tamm's (1991) polarized IR study and calculated order parameter reveal substantial peptide orientation (highly unlikely for a random coil) and thus support the presence of helical structure in the exchanged peptide. Zhang et al. (1992) have also reported the IR spectrum of a synthetic peptide with a fully exchanged helical structure possessing an amide I′ absorbance band near 1644 cm^{-1}. Thus, in the current case the observed frequency reduction in D_2O of ~21 cm^{-1} (from the helical position of 1656 cm^{-1} in H_2O to 1635 cm^{-1}) is clearly too large in magnitude to arise from an exchanged α-helix and implies that a different conformation is present in the monolayer. In addition, the presence of substantial residual amide II intensity near 1550 cm^{-1} for the peptide in both monolayers (Fig. 5) indicates incomplete H→D exchange, which would lead to an amide I frequency decrease of substantially less than 12 cm^{-1} for a helical peptide. Finally, comparison of current relative amide I/II intensities with prior ATR results reported for unexchanged peptide (Brauner et al., 1987) reveals that <~25% exchange has taken place at the air/D_2O interface. To summarize: the absence of significant exchange, together with the observed amide I frequency and bandwidth, strongly suggests that in the presence of both DPPC and DPPS monolayers on a D_2O subphase, the secondary structure of melittin is altered from a predominantly α-helical motif.

It is difficult to ascertain the new secondary structure precisely. Antiparallel β-sheets have their amide I band split into a doublet, with a strong component near 1630 and a much weaker band near 1680 cm^{-1}. The current IRRAS data suggest that part of the observed contour may arise from the low-frequency component of the β-sheet amide I mode, with the weaker high-frequency component obscured in the spectral background. In addition, contributions from turns and unordered or extended forms are certainly plausible in the 1630–1640 cm^{-1} region (Susi and Byler, 1983). The possibility of unordered forms is potentially relevant to the insertion process, because melittin in monomeric form (low concentration) in aqueous solution is indeed unordered (Dempsey, 1990). Because tetrameric melittin is α-helical, it is tempting to infer from the current work that melittin inserted into PC and PS monolayers is at least partially monomeric. In any case, the amide I bandwidth suggests that more than one conformation is present.

Sui et al. (1994) observed (figure 4 in their study) the bulk phase spectrum of melittin in mixed dimyristoyl-PC (DMPC)/DMPA vesicles (D_2O-based buffer) at 45°C. A substantial shoulder appeared at 1637 cm^{-1}, in addition to the main α-helical component of the amide I near 1651 cm^{-1}. Although they did not comment on this feature, it is consistent with the presence of more than one conformation. The current IRRAS result marks the first direct detection at the A/W interface of a well-defined changed conformation for a peptide inserted into a lipid monolayer compared with its insertion into vesicles.

Dempsey et al. (1989) report that in mixed bulk-phase systems, PS stabilizes PC bilayers with respect to the melittin-induced formation of smaller structures, whereas other studies support the induction of peptide-free PC domains (Lafleur et al., 1989). The current monolayer results support the position that the presence of PS offsets the effect that melittin has on PC; i.e., the former induces conformational disordering, the latter substantial conformational ordering.

The general issue of peptide-induced phase separation in mixed lipid systems is of interest. To address these and other topics pertinent to the mechanisms of melittin-induced membrane lysis, future IRRAS studies with improved temperature control and water vapor compensation are likely to be useful.

This work was supported by the Public Health Service through grant GM-29864 to R. M. Funds for spectrometer construction were supplied by Rutgers University.

REFERENCES

Batenburg, A. M., J. C. L. Hibbeln, and B. deKruijff. 1987a. Lipid specific penetration of melittin into phospholipid model membranes. *Biochim. Biophys. Acta.* 903:155–165.

Batenburg, A. M., J. H. vanEsch, J. Leunissen-Bijvelt, A. J. Verkleij, and B. deKruijff. 1987b. Interaction of melittin with negatively charged phospholipids: consequences for lipid organization. *FEBS Lett.* 223: 148–154.

Birdi, K. S., and V. S. Gevod. 1987. Melittin and ionic surfactant interactions in monomolecular films. *Colloid Polym. Sci.* 265:257–261.

Birdi, K. S., V. S. Gevod, O. S. Ksenzhek, E. Stenby, and K. L. Rasmussen. 1983. Equation of state for monomolecular films of melittin at air-water interface. *Colloid Polym. Sci.* 261:767–775.

Brauner, J. W., R. Mendelsohn, and F. G. Prendergast. 1987. Attenuated total reflectance Fourier transform infrared studies of the interaction of melittin, two fragments of melittin, and delta-hemolysin with phosphatidylcholines. *Biochemistry.* 26:8151–8158.

Cornut, I., B. Desbat, and J. Dufourcq. 1995. Detection, structure and orientation of amphipathic peptides and phospholipids on monolayers: an "in situ" approach by PMIRRAS. *Biophys. J.* 68:A213.

Dempsey, C. E. 1990. The action of melittin on membranes. *Biochim. Biophys. Acta.* 1031:143–161.

Dempsey, C., M. Bitbol, and A. Watts. 1989. Interaction of melittin with mixed phospholipid membranes composed of dimyristoylphosphatidylcholine and dimyristoylphosphatidylserine studied by deuterium NMR. *Biochemistry.* 28:6590–6596.

Dluhy, R. A., R. Mendelsohn, H. L. Casal, and H. H. Mantsch. 1983. Interaction of dipalmitoylphosphatidylcholine and dimyristoyl phosphatidylcholine-d_{54} mixtures with glycophorin. A Fourier transform infrared investigation. *Biochemistry.* 22:1170–1177.

Dufourc, E. J., I. C. P. Smith, and J. Dufourcq. 1986. Molecular details of melittin-induced lysis of phospholipid membranes as revealed by deuterium and phosphorus NMR. *Biochemistry.* 25:6448–6455.

Ebara, Y., and Y. Okahata. 1993. In situ surface-detecting technique by using a quartz-crystal microbalance. Interaction behaviors of proteins onto a phospholipid monolayer at the air-water interface. *Langmuir.* 9:574–576.

Flach, C. R., J. W. Brauner, and R. Mendelsohn. 1993a. Calcium ion interactions with insoluble phospholipid monolayer films at the A/W interface. External reflection-absorption studies. *Biophys. J.* 65: 1994–2001.

Flach, C. R., J. W. Brauner, and R. Mendelsohn. 1993b. Coupled external reflectance FT-IR/miniaturized surface film apparatus for biophysical studies. *Appl. Spectrosc.* 47:982–985.

Flach, C. R., J. W. Brauner, J. W. Taylor, R. C. Baldwin, and R. Mendelsohn. 1994. External reflection FTIR of peptide monolayer films in situ at the air/water interface: experimental design, spectra-structure corre-

lations, and effects of hydrogen-deuterium exchange. *Biophys. J.* 67: 402–410.

Frey, S., and L. K. Tamm. 1991. Orientation of melittin in phospholipid bilayers. A polarized attenuated total reflection infrared study. *Biophys. J.* 60:922–930.

Hermetter, A., and J. R. Lakowicz. 1986. The aggregation state of melittin in lipid bilayers. An energy transfer study. *J. Biol. Chem.* 261: 8243–8248.

Hunt, R. D., M. L. Mitchell, and R. A. Dluhy. 1989. The interfacial structure of phospholipid monolayer films: an infrared reflectance study. *J. Mol. Struct.* 214:93–109.

John, E., and F. Jahnig. 1991. Aggregation state of melittin in lipid vesicle membranes. *Biophys. J.* 60:319–328.

Jones, M. N., and D. Chapman. 1995. Micelles, Monolayers, and Biomembranes. Wiley-Liss, New York.

Lafleur, M., J. Faucon, J. Dufourcq, and M. Pezolet. 1989. Perturbation of binary phospholipid mixtures by melittin: a fluorescence and Raman spectroscopy study. *Biochim. Biophys. Acta.* 980:85–92.

Mendelsohn, R., J. W. Brauner, and A. Gericke. 1995. External infrared reflection absorption spectrometry of monolayer films at the air/water interface. *Annu. Rev. Phys. Chem.* 46:305–334.

Mendelsohn, R., R. Dluhy, T. Taraschi, D. G. Cameron, and H. H. Mantsch. 1981. Raman and Fourier transform infrared spectroscopic studies of the interaction between glycophorin and dimyristoylphosphatidylcholine. *Biochemistry.* 20:6699–6706.

Miyazawa, T., T. Shimanouchi, and S.-I. Mizushima. 1958. Normal vibrations of *N*-methylacetamide. *J. Chem. Phys.* 29:611–616.

Ohki, S., E. Marcus, D. K. Sukumaran, and K. Arnold. 1994. Interaction of melittin with lipid membranes. *Biochim. Biophys. Acta.* 1194:223–232.

Okada, A., K. Wakamatsu, T. Miyazawa, and T. Higashijima. 1994. Vesicle-bound conformation of melittin: transferred nuclear Overhauser enhancement analysis in the presence of perdeuterated phosphatidylcholine vesicles. *Biochemistry.* 33:9438–9446.

Pastrana-Rios, B., A. J. Mautone, S. Taneva, K. M. W. Keough, and R. Mendelsohn. 1996. An IRRAS study of lung surfactant SP-B and SP-C in phospholipid monolayers at the A/W interface. *Biophys. J.* In press.

Pezolet, M., and J. Labrecque. 1995. Surface pressure modulation of the conformation of poly(L-lysine) bound to phospholipid monolayers. *Biophys. J.* 68:A213.

Smith, R., F. Separovic, F. C. Bennett, and B. A. Cornell. 1992. Melittin-induced changes in lipid multilayers. A solid-state NMR study. *Biophys. J.* 63:469–474.

Smith, R., F. Separovic, T. J. Milne, A. Whittker, F. M. Bennett, B. A. Cornell, and A. Makriyannis. 1994. Structure and orientation of the pore-forming peptide, melittin, in lipid bilayers. *J. Mol. Biol.* 241: 456–466.

Snyder, R. G., H. L. Strauss, and C. A. Elliger. 1982. C-H stretching modes and the structure of *n*-alkyl chains. 1. Long, disordered chains. *J. Phys. Chem.* 86:5145–5150.

Sui, S., H. Wu, Y. Guo, and K. Chen. 1994. Conformational changes of melittin upon insertion into phospholipid monolayer and vesicle. *J. Biochem.* 116:482–487.

Susi, H., and D. M. Byler. 1983. Protein structure by Fourier transform infrared spectroscopy: second derivative spectra. *Biochem. Biophys. Res. Commun.* 115:391–397.

Vogel, H., F. Jahnig, V. Hoffmann, and J. Stumpel. 1983. The orientation of melittin in lipid membranes. A polarized infrared spectroscopy study. *Biochim. Biophys. Acta.* 733:201–209.

Weaver, A. J., M. D. Kemple, J. W. Brauner, R. Mendelsohn, and F. G. Prendergast. 1992. Fluorescence, CD, attenuated total reflectance (ATR) FTIR, and ^{13}C NMR characterization of the structure and dynamics of synthetic melittin and melittin analogues in lipid environments. *Biochemistry.* 31:1301–1313.

Zhang, Y.-P., R. N. A. H. Lewis, R. S. Hodges, and R. N. McElhaney. 1992. FTIR spectroscopic studies of the conformation and amide hydrogen exchange of a peptide model of the hydrophobic transmembrane α-helices of membrane proteins. *Biochemistry.* 31:11572–11578.